


# Interferon- $\lambda$ Enhances the Differentiation of Naive B Cells into Plasmablasts via the mTORC1 Pathway

## Journal Article

**Author(s):**

Syedbasha, Mohammedyaseen; Bonfiglio, Ferdinando; [Linnik, Janina Esther](#) ; Stühler, Claudia; Wüthrich, Daniel; Egli, Adrian

**Publication date:**

2020-10-06

**Permanent link:**

<https://doi.org/https://doi.org/10.3929/ethz-b-000445399>

**Rights / license:**

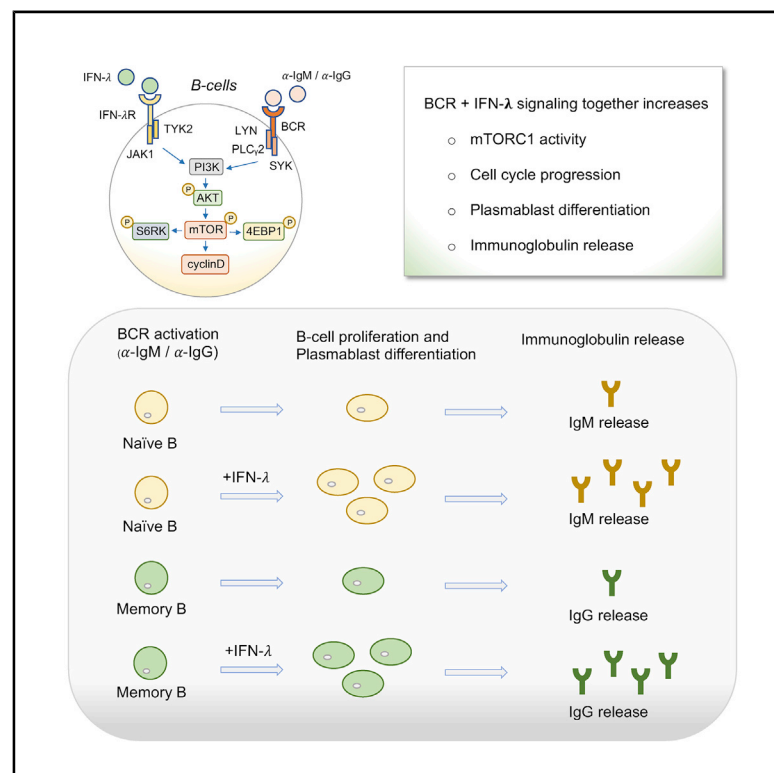
[Creative Commons Attribution 4.0 International](#)

**Originally published in:**

Cell Reports 33(1), <https://doi.org/10.1016/j.celrep.2020.108211>

# Interferon- $\lambda$ Enhances the Differentiation of Naive B Cells into Plasmablasts via the mTORC1 Pathway

## Graphical Abstract



## Authors

Mohammedyaseen Syedbasha, Ferdinando Bonfiglio, Janina Linnik, Claudia Stuehler, Daniel Wüthrich, Adrian Egli

## Correspondence

m.syedbasha@unibas.ch (M.S.),  
adrian.egli@usb.ch (A.E.)

## In Brief

Syedbasha et al. show that IFN- $\lambda$  signaling works synergistically with BCR signaling and boosts B cell differentiation by enhancing mTORC1 activity and cell-cycle progression. Understanding this molecular mechanism may help to improve vaccine efficacy and optimize treatment strategies to target the immune cells involved in autoimmunity.

## Highlights

- IFN- $\lambda$  induces long-lasting and cell-type-specific gene expression in B cells
- IFN- $\lambda$  raises the expression of mTORC1, MYC, and inflammatory-response-related gene sets
- IFN- $\lambda$  increases cell-cycle progression in B cells upon BCR activation
- IFN- $\lambda$  enhances plasmablast differentiation upon BCR activation



## Report

# Interferon- $\lambda$ Enhances the Differentiation of Naive B Cells into Plasmablasts via the mTORC1 Pathway

Mohammedyaseen Syedbasha,<sup>1,6,\*</sup> Ferdinando Bonfiglio,<sup>1,2</sup> Janina Linnik,<sup>2,3</sup> Claudia Stuehler,<sup>4</sup> Daniel Wüthrich,<sup>1,2,5</sup> and Adrian Egli<sup>1,5,\*</sup>

<sup>1</sup>Applied Microbiology Research, Department of Biomedicine, University of Basel, Basel, Switzerland

<sup>2</sup>Swiss Institute for Bioinformatics, Basel, Switzerland

<sup>3</sup>Department of Biosystems Science and Engineering, ETH Zurich, Basel, Switzerland

<sup>4</sup>Infection Biology Laboratory, Department of Biomedicine, University of Basel, Basel, Switzerland

<sup>5</sup>Clinical Bacteriology and Mycology, University Hospital Basel, Basel, Switzerland

<sup>6</sup>Lead Contact

\*Correspondence: [m.syedbasha@unibas.ch](mailto:m.syedbasha@unibas.ch) (M.S.), [adrian.egli@usb.ch](mailto:adrian.egli@usb.ch) (A.E.)

<https://doi.org/10.1016/j.celrep.2020.108211>

## SUMMARY

Type III interferon (interferon lambda [IFN- $\lambda$ ]) is known to be a potential immune modulator, but the mechanisms behind its immune-modulatory functions and its impact on plasmablast differentiation in humans remain unknown. Human B cells and their subtypes directly respond to IFN- $\lambda$ . Using B cell transcriptome profiling, we investigate the immune-modulatory role of IFN- $\lambda$  in B cells. We find that IFN- $\lambda$ -induced gene expression in B cells is steady, prolonged, and importantly, cell type specific. Furthermore, IFN- $\lambda$  enhances the mTORC1 (mammalian/mechanistic target of rapamycin complex 1) pathway in B cells activated by the B cell receptor (BCR/anti-IgM). Engagement of mTORC1 by BCR and IFN- $\lambda$  induces cell-cycle progress in B cells. Subsequently, IFN- $\lambda$  boosts the differentiation of naive B cells into plasmablasts upon activation, and the cells gain effector functions such as cytokine release (IL-6 and IL-10) and antibody production. Our study shows how IFN- $\lambda$  systematically boosts the differentiation of naive B cells into plasmablasts by enhancing the mTORC1 pathway and cell-cycle progression in activated B cells.

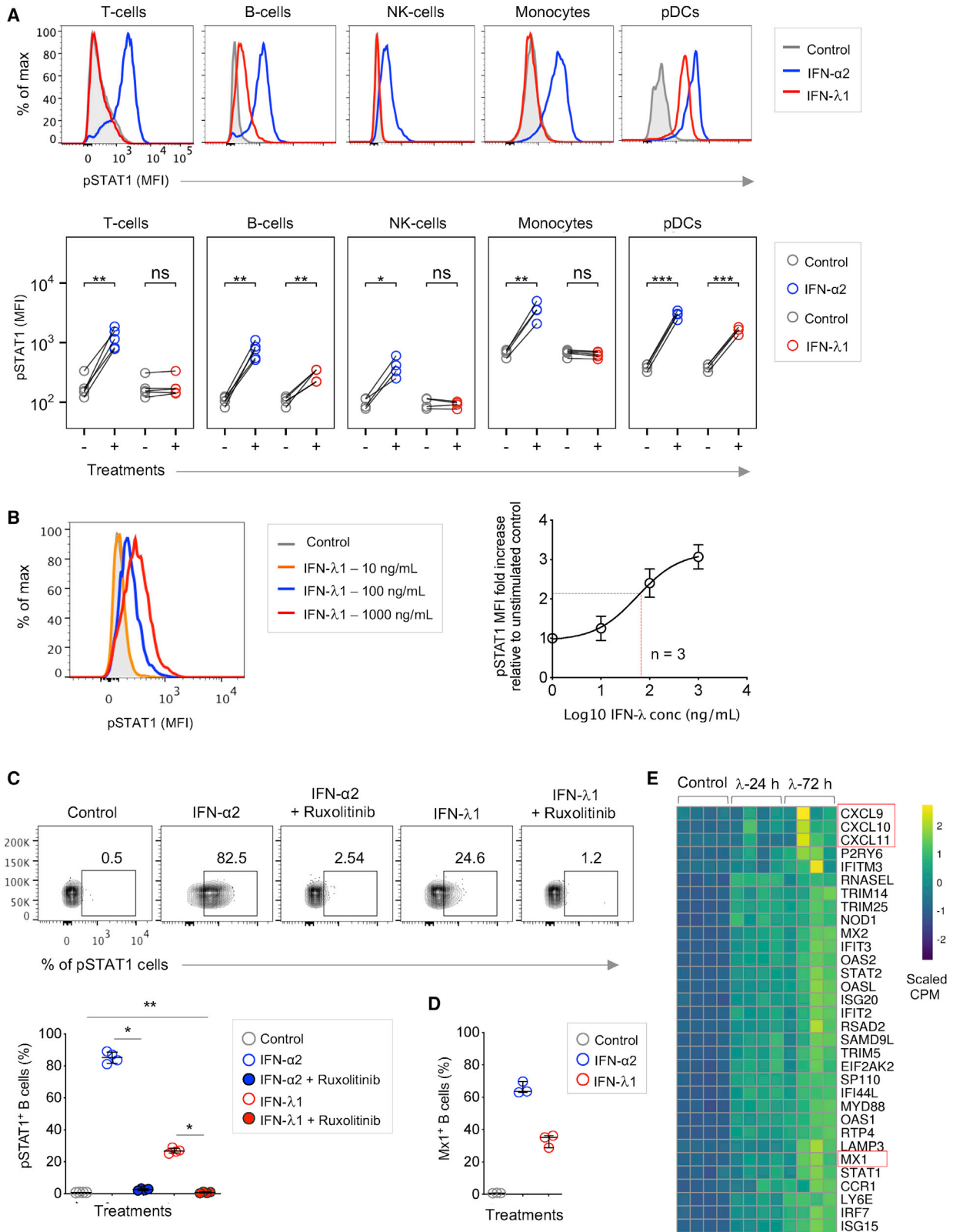
## INTRODUCTION

Type III interferons (IFNs), or the interferon lambda (IFN- $\lambda$ ) family, are crucial antiviral effectors. IFN- $\lambda$ -mediated immunity is not only limited to viruses such as hepatitis C virus (HCV), human immunodeficiency virus (HIV), influenza, norovirus, West Nile virus (WNV), and Zika virus but also extends to other pathogens, such as bacteria, parasites, and fungi (Caine et al., 2019; Galani et al., 2017; Lazear et al., 2015; Nice et al., 2015; Syedbasha and Egli, 2017). The IFN- $\lambda$  family consists of four members: IFN- $\lambda$ 1, IFN- $\lambda$ 2, IFN- $\lambda$ 3, and IFN- $\lambda$ 4. They bind to a heterodimeric surface receptor, which is composed of the ubiquitously expressed interleukin (IL) 10 receptor beta (IL10R $\beta$ ) chain and the unique IFN- $\lambda$  receptor 1 (IFNLR1) chain. Receptor binding activates the Janus kinase signal transducer and activator of transcription (JAK-STAT) pathway and induces the expression of hundreds of IFN-stimulated genes (ISGs) (Egli et al., 2014). The IFN- $\alpha/\beta$  receptor (type I) and the IFN- $\gamma$  receptor (type II) are expressed in nearly every cell type (Schneider et al., 2014). In contrast, expression of the IFN- $\lambda$  receptor is limited to hepatocytes, epithelial cells, and a few immune cell types (Doyle et al., 2006; Pott et al., 2011; Syedbasha and Egli, 2017). Cell-specific receptor expression and signaling kinetics make IFN- $\lambda$  unique compared with other IFNs (Marcello et al., 2006). In mouse immune cells, neutrophils and CD103+ dendritic cells (DCs) are shown to directly respond to

IFN- $\lambda$  (Broggi et al., 2017; Hemann et al., 2019). In human immune cells, however, many contradictory data have been reported on the expression of the IFN- $\lambda$  receptor. This is mainly because of the low level of receptor expression, low assay sensitivity, and lack of receptor-specific antibodies to detect the functional IFN- $\lambda$  receptor. Moreover, impurities in immune cell isolation and detection of the IFN- $\lambda$  receptor in the mRNA level by quantitative PCR (qPCR) can provide misleading data on expression of the functional IFN- $\lambda$  receptor in the specific immune cell subtype. In brief, plasmacytoid dendritic cells (pDCs) have been shown to strongly express the IFN- $\lambda$  receptor, whereas direct response of other immune cells to IFN- $\lambda$  is the subject of long-standing debates (Ank et al., 2008; Dai et al., 2009; de Groen et al., 2015; Dickensheets et al., 2013; Gallagher et al., 2010; Kelly et al., 2016; Megjugorac et al., 2009; Witte et al., 2009). Understanding of which immune cells respond to IFN- $\lambda$  is critical to further study the impact of IFN- $\lambda$  in cellular functions.

IFN- $\lambda$  is secreted by many cell types, including DCs, following infection or vaccination (Wack et al., 2015; Zhang et al., 2013). Triggering of the B cell receptor (BCR) by extracellular antigens or ligands promotes resting naive/memory B cells to proliferate and differentiate into antibody-secreting cells (ASCs). Activation of BCR signals instructs B cells to make crucial cell-fate decisions. The B cell differentiation process is linked to a certain number of cell divisions that are necessary to allow the expression of





(legend on next page)

transcription factors such as Blimp1 (B lymphocyte-induced maturation protein-1) and IRF4 (IFN regulatory factor 4) (Tellier et al., 2016). During this process, the phenotypic changes take place in naive/memory B cells and the cells gain additional functions such as protein secretion (Lou et al., 2015). The T cells release cytokines including IL-5 (in mouse) and IL-21 (in humans), which are known to enhance plasmablast differentiation (Chevrier et al., 2009; Moens and Tangye, 2014). In this context of B cell differentiation, the role of IFN- $\lambda$  is not known.

In this study, we first show the specific responsiveness of various immune cell populations to IFN- $\lambda$ , using a highly sensitive phospho-flow cytometry assay. Next, we performed B cell transcriptome profiling, and finally, we follow-up *in vitro* assays to investigate the immune-modulatory role of IFN- $\lambda$  in B cells and their subtypes. Our data systematically indicate that similar to type I IFNs, IFN- $\lambda$  boosts the differentiation of naive B cells into plasmablasts by enhancing the mammalian/mechanistic target of rapamycin complex 1 (mTORC1) signaling pathway and cell-cycle progression in BCR-activated B cells.

## RESULTS

### Immune Cell-Specific Response to IFN- $\lambda$

We investigated the specific responsiveness of various immune cell subtypes to IFN- $\lambda$  by phospho-flow cytometry assay. To investigate whether IFN- $\lambda$  signals through a JAK-STAT pathway to stimulate gene expression, like type I IFNs such as IFN- $\alpha$  or IFN- $\beta$  (Horvath, 2004), IFN- $\alpha 2$  was used as a positive control in the following assays. First, we quantified STAT1 phosphorylation (pSTAT1) induced by IFN- $\alpha 2$  (1,000 U/mL) or IFN- $\lambda 1$  (1  $\mu$ g/mL) in peripheral blood mononuclear cells (PBMCs) using phospho-flow cytometry. All analyzed immune cell subtypes from PBMCs, i.e., T cells (CD3, CD4, and CD8), B cells, natural killer (NK) cells, monocytes, and pDCs, responded to IFN- $\alpha 2$ . Remarkably, B cells and pDCs responded to IFN- $\lambda 1$ , but not other cell subtypes (Figure 1A; Figure S1A). Comparatively, pDCs showed more response to IFN- $\lambda 1$  than did B cells (Figure S1B). Similarly, we measured IFN- $\alpha 2$ - or IFN- $\lambda 1$ -induced STAT2 phosphorylation in isolated B cells using phospho-flow cytometry (Figure S1C). Independent of flow cytometry analysis, we confirmed the responsiveness of B cells to IFN- $\lambda 1$  by western blot with pSTAT1 measurement (Figure S1D). IFN- $\lambda 1$  induced STAT1 phosphorylation in a dose-dependent manner with a half maximal effective concentration (EC<sub>50</sub>) of about 56 ng/mL (Figure 1B). Furthermore, IFN- $\lambda 2$  and IFN- $\lambda 3$  induced pSTAT1 in a manner similar to IFN- $\lambda 1$

in B cells (Figure S1E). We then investigated isolated B cells to compare the level of STAT1 phosphorylation induced by IFN- $\lambda 1$  within B cell subpopulations. The IFN- $\lambda 1$ -induced pSTAT1 level is slightly higher in naive B cells compared with CD27<sup>+</sup> memory B cells (Figure S1F). A JAK inhibitor assay was used to confirm that IFN- $\lambda$  signals through the JAK-STAT pathway: the JAK inhibitor (3  $\mu$ M ruxolitinib) almost blocked IFN- $\alpha 2$ - or IFN- $\lambda 1$ -induced STAT1 phosphorylation in isolated B cells (Figure 1C). IFN- $\lambda$ -induced gene expression was confirmed with Mx1 (MX dynamin-like guanosine triphosphatase [GTPase] 1) measurement at 24 h by flow cytometry (Figure 1D). The Mx1-encoded protein is induced by type I and type II IFNs against a range of viruses (Haller et al., 2018). The B cell gene expression from transcriptome analysis showed that IFN- $\lambda$ -induced expression of ISGs increased over 72 h, including chemokines such as CXCL9, CXCL10, and CXCL11 (highlighted by the red box) in B cells (Figure 1E). So IFN- $\lambda$  directly induces the ISG expression in human B cells via the JAK-STAT signaling pathway.

### IFN- $\lambda$ Elevates the BCR-Induced mTORC1 Pathway

To understand the immune-modulatory effect of IFN- $\lambda$  with B cell fate and function, we isolated the B cell population via fluorescence-activated cell sorting (FACS) (gating strategy outlined in Figure S2A) and performed B cell transcriptional profiling using RNA sequencing (RNA-seq) (schematic workflow described in Figure S2B). The number of dysregulated genes in each stimulation condition are shown in Figure S2C (marked with red dots). Interestingly, 271 genes were further altered by IFN- $\lambda 3$  over stimulation with the immunoglobulin (Ig)  $\alpha$ -IgM (Fab'2 fragment). We performed a gene set enrichment analysis to identify the pathways enriched by IFN- $\lambda$  and during BCR activation (Table S1). The metabolic pathway (mTORC1 and MYC) and gene sets related to the cell cycle (E2F and G2M) were highly enriched following the gene sets (commonly shared) of IFN- $\alpha$  or IFN- $\gamma$  responses. The expression of E2F, G2M, and mTORC1-related genes was higher when IFN- $\lambda$  was added with BCR activation compared with IFN- $\lambda$  alone (Tables S1 and S2).

Based on this finding, we first wanted to explore the mTORC1 signaling pathway. The genes involved in mTORC1 signaling were significantly upregulated under the  $\alpha$ -IgM + IFN- $\lambda 3$  condition compared with  $\alpha$ -IgM alone (Figure 2A). To verify the effect of IFN- $\lambda$  on mTORC1 signaling in BCR-activated B cells, the phosphorylation of well-established mTORC1 targets ribosomal protein S6 (S235/p236) and eukaryotic translation initiation factor 4E-binding protein 1 (4EBP1) (T37/46), along with mTORC1

### Figure 1. Immune Cell-Specific Response to IFN- $\lambda$

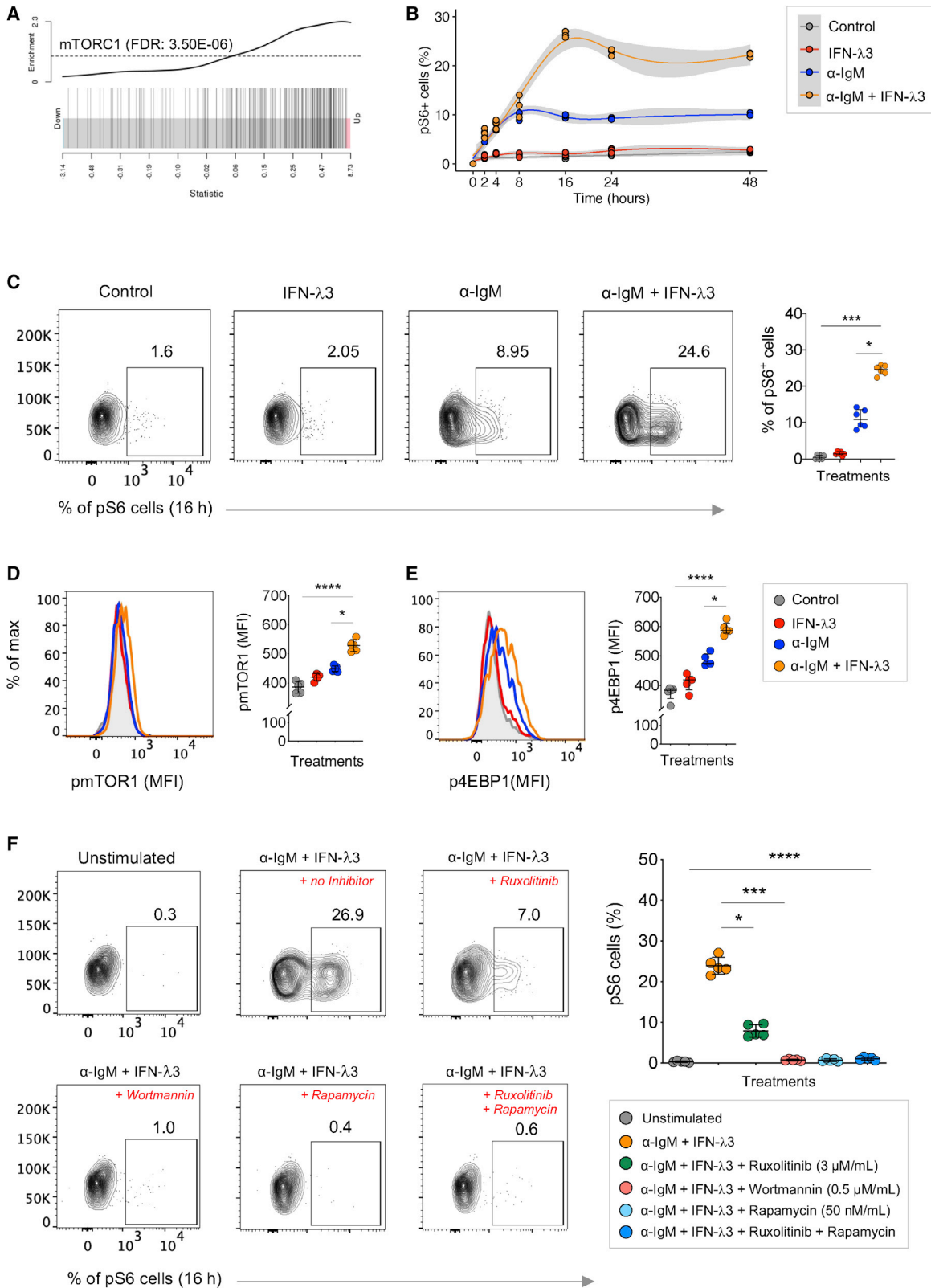
(A) Phospho-flow cytometry analysis was performed to quantify the phosphorylation of STAT1 upon IFN- $\alpha 2$  or IFN- $\lambda 1$  stimulation in PBMCs (for 30 min) from 4 to 5 healthy donors. In the upper row, the representative FACS histogram plot with the geometric mean fluorescence intensity (MFI) of pSTAT1 induction is shown for each subpopulation from PBMCs (T cells, CD3; B cells, CD19; NK cells, Nkp46; monocytes, CD14; pDCs, CD123 and BDCA-2). The collective donors of corresponding subpopulations are shown below. Statistical significance was determined using a paired two-tailed Student's t test on the log-transformed MFI values and Benjamini-Krieger-Yekutieli (BKY) correction for multiple comparisons: \*p < 0.05, \*\*p < 0.01, \*\*\*p < 0.001.

(B) Dose-responsive induction of pSTAT1 in B cells. IFN- $\lambda 1$  induced STAT1 phosphorylation in B cells in a dose-dependent manner (n = 3, EC<sub>50</sub> = 56.1 ng/mL).

(C) Isolated B cells pretreated (for 30 min) with ruxolitinib (3  $\mu$ M/mL) were unstimulated or stimulated with IFN- $\alpha 2$  or IFN- $\lambda 1$  for 30 min. Induction of STAT1 phosphorylation was measured, and statistical significance was determined using a non-parametric ANOVA (Kruskal-Wallis) test and BKY correction for multiple comparisons: \*p < 0.05, \*\*p < 0.01, \*\*\*p < 0.001. Data are shown as median with interquartile range (IQR) (n = 4).

(D) Expression of Mx1 was measured in isolated B cells after 24 h of stimulation with IFN- $\alpha 2$  or IFN- $\lambda 1$  using flow cytometry (n = 3).

(E) Heatmap of IFN-stimulated gene (ISG) expression in B cells by IFN- $\lambda 3$  for 24 and 72 h. The expression of genes is shown in mRNA copies in counts per million (CPM).



(legend on next page)

(S2448), was assessed (Hay and Sonenberg, 2004). IFN- $\alpha$ 2 was included in this experiment to compare the effect of type III IFN with type I IFN signaling on the mTORC1 pathway. First, we quantified the phosphorylation of S6 induced by IFN- $\lambda$ 3/IFN- $\alpha$ 2,  $\alpha$ -IgM, or  $\alpha$ -IgM and IFN- $\lambda$ 3/IFN- $\alpha$ 2 in combination over a time course of 48 h in isolated B cells. We found that IFN- $\lambda$ 3 or IFN- $\alpha$ 2 alone did not increase S6 phosphorylation (Figure 2B; Figure S2D). Without additional induction, only BCR-induced S6 phosphorylation was increased gradually up to 8 h and sustained over 48 h. IFN- $\lambda$ 3 significantly enhanced BCR-induced S6 phosphorylation over 16 h, similar to IFN- $\alpha$ 2, and then slightly reduced over 48 h (Figure 2B; Figure S2D). The number of phosphorylated ribosomal protein S6 (pS6)-positive cells increased from approximately 10% to 25% from  $\alpha$ -IgM to  $\alpha$ -IgM with the IFN- $\lambda$ 3 condition, respectively, at 16 h on total B cells (Figure 2C). Likewise, IFN- $\lambda$ 3 enhanced BCR-induced S6 phosphorylation on B cell subpopulations such as naive B cells and non-class-switched and class-switched memory B cells. The responsiveness of naive B cells was marginally higher (about 30% of pS6+ cells) compared with memory B cells (about 25% of pS6+ cells) (Figure S2E). Next, we focused on the phosphorylation of other mTORC1 candidates (mTORC1 and 4EBP1), along with S6, at 16 h. As expected, IFN- $\lambda$ 3 significantly increased BCR-induced phosphorylation of mTORC1 and 4EBP1, along with S6, as measured at 16 h (Figures 2D and 2E).

Finally, we performed checkpoint inhibitor assays to confirm stimuli-specific induction of the mTORC1 pathway by pS6 quantification at 16 h. Inhibition of mTORC1 by rapamycin blocks S6 phosphorylation by  $\alpha$ -IgM + IFN- $\lambda$ 3, whereas inhibition of IFN- $\lambda$  signaling by ruxolitinib (a JAK1/2 inhibitor) blocks the IFN- $\lambda$ -induced boost of S6 phosphorylation. Moreover, inhibition of phosphatidylinositol 3-kinase (PI3K) by wortmannin blocks S6 phosphorylation, which confirms that BCR-induced activation of mTORC1 acts via PI3K (Figure 2F) (Munakata and Tobinai, 2018).

### IFN- $\lambda$ Increases BCR-Induced Cell-Cycle Progression in B Cells

mTORC1 controls cell proliferation and cell growth by modulating mRNA translation via the phosphorylation of downstream targets like 4EBP1 to 4EBP3 and S6 kinases (Dowling et al., 2010). Because IFN- $\lambda$  boosted the phosphorylation of BCR-induced mTORC1 downstream targets S6 and 4EBP1, we

sought to identify whether IFN- $\lambda$  can increase the BCR-induced cell cycle. The gene set enrichment analysis indicated that E2F targets (false discovery rate [FDR] = 5.44E-19) and G2M checkpoint genes (FDR = 1.17E-15) involved in the cell-cycle process were significantly upregulated in  $\alpha$ -IgM with the IFN- $\lambda$ 3 condition compared with  $\alpha$ -IgM alone (Figures 3A and 3B). In addition, significant upregulation of genes involved in cell-cycle-related biological processes was observed when testing the enrichment against the Gene Ontology (GO) database (Figure 3C).

To verify the influence of IFN- $\lambda$  in the cell cycle of BCR-activated cells, we measured Ki-67 in isolated B cells. The expression of Ki-67 is associated with cell proliferation, and it increases during the S phase of the cell cycle (Darzynkiewicz et al., 2015). As expected, IFN- $\lambda$ 3 and IFN- $\alpha$ 2 notably increased the expression Ki-67 in  $\alpha$ -IgM with the IFN- $\lambda$ 3 or IFN- $\alpha$ 2 condition compared with  $\alpha$ -IgM alone. The number of Ki-67+ cells increased from 12% ( $\alpha$ -IgM) to 30% ( $\alpha$ -IgM + IFN- $\lambda$ 3) (Figure 3D; Figure S3A). However, either IFN- $\lambda$ 3 or IFN- $\alpha$ 2 alone did not induce Ki-67 expression. Collectively, the data show that among the B cell subpopulations, naive B cells showed a better response (Figure S3B).

In addition, we performed proliferation assays with CellTrace violet (CTV)-labeled and sorted B cells and their subpopulations. IFN- $\lambda$ 3 or IFN- $\alpha$ 2 alone failed to induce the proliferation of B cells, whereas activation of B cells with  $\alpha$ -IgM induced proliferation. The proliferative response of BCR-activated B cells was significantly increased 2-fold by IFN- $\lambda$ 3 or IFN- $\alpha$ 2 on total B cells (Figure 3E; Figure S3C). Among B cell subtypes, the proliferation of naive B cells increased up to 40% with the  $\alpha$ -IgM + IFN- $\lambda$ 3 condition, whereas memory B cell proliferation increased about 30% compared with the unstimulated control (Figure S3D). The inhibition of mTORC1 by rapamycin blocks the proliferation induced by  $\alpha$ -IgM + IFN- $\lambda$ 3, whereas the inhibition of IFN- $\lambda$  signaling by ruxolitinib blocks only the IFN- $\lambda$ -induced boost of proliferation, not IgM-induced proliferation (Figure 3E). The gating strategy for sorting B cells and their subpopulations is shown in Figure S3E. Overall viability of the cells was assessed under these different stimulation conditions (Figure S3F).

### Effect of IFN- $\lambda$ on Differentiation of Naive B Cells into Plasmablasts

Activation of mTORC1 and cell-cycle progression can promote the cellular differentiation process (Fruman et al., 2017). To

#### Figure 2. IFN- $\lambda$ Elevates the BCR-Induced mTORC1 Pathway

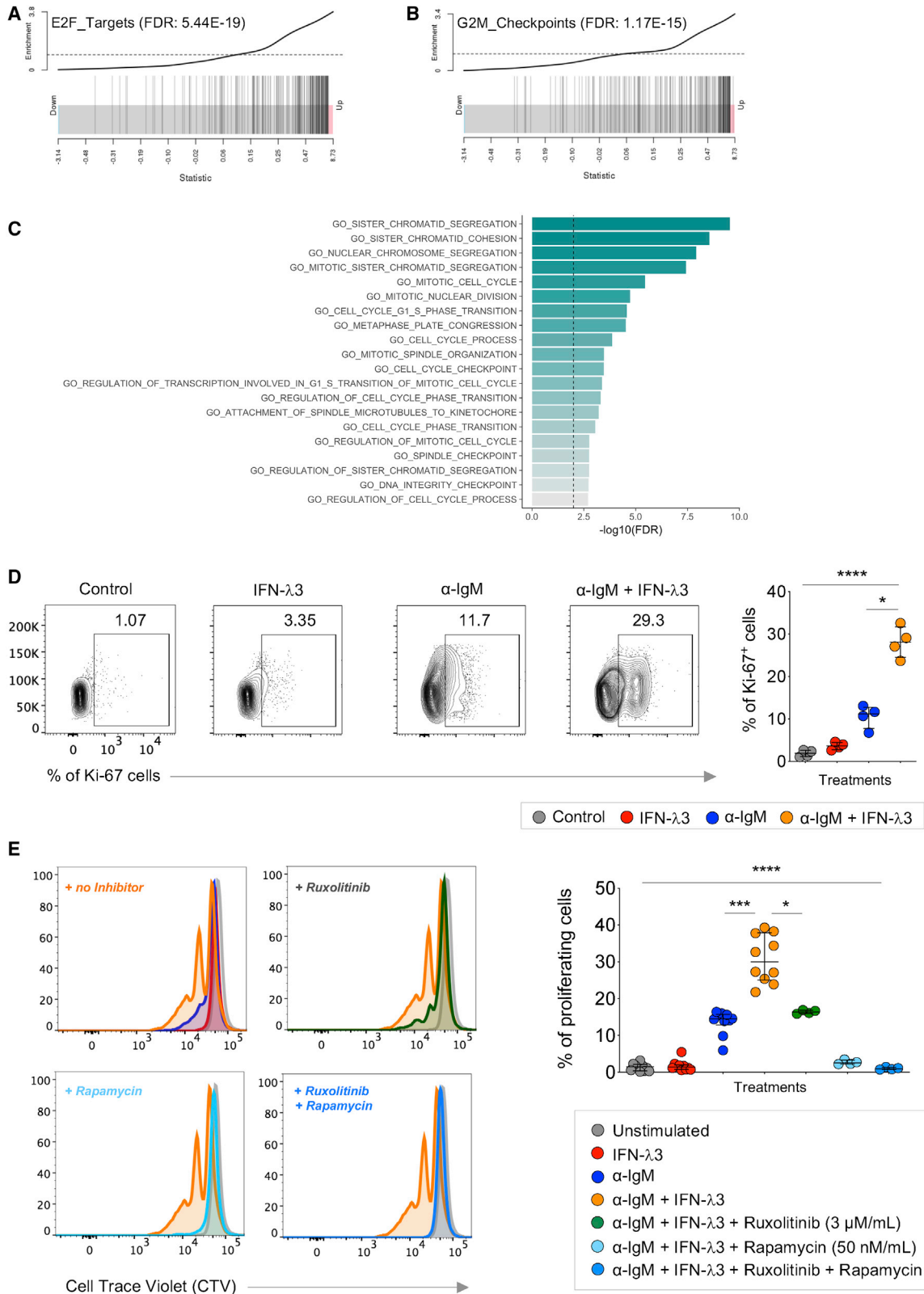
(A) Hallmark gene set enrichment barcode plot showing mTORC1 signaling genes to be relatively more activated by IFN- $\lambda$ 3 in the  $\alpha$ -IgM + IFN- $\lambda$ 3 condition compared with  $\alpha$ -IgM alone (FDR = 3.50E-6). The log fold change (FC) is ranked left to right from smallest to largest. The ranked statistics are represented by shaded bars, and the positions of the specified subsets are marked by vertical bars. The enrichment worm (top) shows the relative enrichment of the vertical bars in each part of the plot.

(B) Purified B cells were stimulated with IFN- $\lambda$ 3/IFN- $\alpha$ 2,  $\alpha$ -IgM, or the combination of  $\alpha$ -IgM with IFN- $\lambda$ 3/IFN- $\alpha$ 2 over a 48 h time course to quantify the mTORC1 target protein, S6 phosphorylation (Ser235/236) (n = 3). A linear smoothing spline has been fitted to each treatment (lines show fits, and shaded areas indicate 95% confidence intervals). The error bars indicate the standard deviation.

(C) Left: representative FACS plot. The data show the phosphorylation of S6 upon stimulation after 16 h. Right: percentage of pS6+ cells from collective donors (n = 6). Data show median and IQR. Significance was determined using a non-parametric ANOVA (Kruskal-Wallis) test: \*p < 0.05, \*\*p < 0.01, \*\*\*p < 0.001.

(D and E) Phosphorylation of different targets of the mTORC1 pathway, pmTOR1 (S2448) and p4EBP1 (T37/46), was quantified at 16 h by flow cytometry. To measure IFN- $\lambda$ 3-induced phosphorylation increase (in geometric mean fluorescence intensity),  $\alpha$ -IgM + IFN- $\lambda$ 3 was compared with the  $\alpha$ -IgM condition by an ANOVA (Tukey) test (after log-transformed MFI values for which normality can be assumed).

(F) Checkpoint inhibitor assays were performed to confirm the stimuli-specific induction of the mTORC1 pathway by quantification of S6 phosphorylation at 16 h. Percentage of pS6 induction is shown. Bars indicate median with IQR (n = 5). Significance was determined by a non-parametric ANOVA (Kruskal-Wallis) test with BKY correction.



(legend on next page)

identify the functional role of IFN- $\lambda$  in B cell differentiation, we performed gene set enrichment analysis on the transcriptomic data. The top 10 hits of immunological signature gene sets are shown in Figure 4A. Genes involved in differentiation of naive B cells into plasmablasts were strongly upregulated when stimulated with  $\alpha$ -IgM + IFN- $\lambda$ 3 compared with  $\alpha$ -IgM alone (FDR =  $4.38E-163$ ) (Figure 4B). It is known that the transcription factors IRF4 and Blimp1 are essential for the differentiation of B cells into ASCs and that IRF4 initiates the differentiation process by activating the PRDM1 gene, which encodes the Blimp1 protein (Kwon et al., 2009). The upregulation of PRDM1 and IRF4 was observed under  $\alpha$ -IgM + IFN- $\lambda$ 3 stimulation, compared with  $\alpha$ -IgM alone, in total B cells by qPCR and FACS intracellular staining, respectively (Figures S4A and S4B).

To confirm the specific effect of IFN- $\lambda$  in differentiation of naive B cells into plasmablasts, we performed the following *in vitro* assays with sorted naive B cells. First, we measured the changes in the phenotypic markers CD27, CD38, CD71, and CD19, as described previously (Ellebedy et al., 2016; Jego et al., 2003). The naive B cells were stimulated with IFN- $\lambda$ 3,  $\alpha$ -IgM, or  $\alpha$ -IgM + IFN- $\lambda$ 3. After 4 days, changes in surface markers were quantified by flow cytometry. The CD38<sup>+</sup>IgM<sup>+</sup> cells increased more than 50% after 4 days of IFN- $\lambda$ 3 with BCR activation (Figure S4C). The expression of surface markers CD71, CD38, and CD27 was found to be significantly increased under  $\alpha$ -IgM + IFN- $\lambda$ 3 stimulation compared with  $\alpha$ -IgM alone. Besides, expression of CD19 was downregulated under the  $\alpha$ -IgM + IFN- $\lambda$ 3 condition (Figure 4C). A similar effect was observed after 4 days of IFN- $\alpha$ 2 with BCR activation (Figure S4D). In addition, increase of the IL-6 receptor (IL-6R) was observed over 4 days under the  $\alpha$ -IgM,  $\alpha$ -IgM + IFN- $\lambda$ 3, and  $\alpha$ -IgM + IFN- $\alpha$ 2 conditions compared with the unstimulated control. However, IFN- $\lambda$ 3 with  $\alpha$ -IgM did not further increase the expression of IL-6R compared with  $\alpha$ -IgM alone (Figure S4E).

Next, we examined the effector functions of BCR- and IFN- $\lambda$ 3/IFN- $\alpha$ 2-activated cells on the B cell differentiation process. The release of IL-6 and IL-10 was greatly induced by IFN- $\lambda$ 3 or IFN- $\alpha$ 2 under the BCR-activated condition (72 h), but IFN- $\lambda$ 3 or IFN- $\alpha$ 2 alone failed to induce cytokines. The JAK and mTORC1 inhibitors could potentially block the release of these cytokines (Figure 4D; Figure S4F). In contrast, no release of other cytokines, i.e., IL-4, IFN- $\gamma$ , tumor necrosis factor (TNF)- $\alpha$ , IL-13, IL-2, TNF- $\beta$ , IL-17A, IL-12p70, A proliferation-inducing ligand (APRIL), B cell-activating factor (BAFF), and CD40L, was observed under other stimulation conditions. A similar result was seen in the release of IL-6 or IL-10 when total B cells or non-class-switched or class-switched-memory B cells were

subjected to these stimulation conditions (IFN- $\lambda$  alone,  $\alpha$ -IgM/ $\alpha$ -IgG alone, and  $\alpha$ -IgM + IFN- $\lambda$ 3/ $\alpha$ -IgG + IFN- $\lambda$ 3) (Figures S4G–S4I).

Lastly, we measured the Ig from supernatants collected (at day five) from BCR- and IFN- $\lambda$ 3-activated naive B cells, cultured with or without mTORC1 checkpoint inhibitors. The analysis was performed using a multi-analyte human Ig isotyping kit. IFN- $\lambda$ 3 was found to boost the release of IgM from BCR-activated cells without inhibitors (Figure 4E). At the same time, no release of IgD, IgA, or IgG1–IgG4 under stimulation conditions was noticed, which indicates that IFN- $\lambda$ 3 in combination with anti-IgM enhances the differentiation of naive B cells into IgM-releasing plasmablasts. A similar response was seen with IgM release by type I IFN (Figures S5A and S5B). PI3K inhibitor wortmannin and mTORC1 inhibitor rapamycin both blocked IgM release, whereas JAK1/2 inhibitor ruxolitinib only reduced the IFN- $\lambda$ 3-induced boost of IgM release by blocking IFN- $\lambda$  signaling independent of BCR response (Figure 4E). Overall, these data suggest that IFN- $\lambda$  boosts the differentiation of naive B cells into IgM-releasing plasmablasts by enhancing the mTORC1 pathway. Furthermore, IFN- $\lambda$ 3 slightly increased the release of IgA and IgG1 along with IgM in BCR-activated memory B cells or total B cells (Figures S5C–S5E). However, IFN- $\lambda$ 3 or  $\alpha$ -IgM alone could increase the expression of the AICDA (activation-induced cytidine deaminase) gene in naive B cells (Figure S5F). Overall, viability of the cells in cytokine (72 h) and Ig (5 days) release assays was assessed under these different stimulation conditions (Figures S4J and S5G).

## DISCUSSION

In this study, we demonstrate the direct responsiveness of B cells to IFN- $\lambda$  using different functional techniques. This allowed us to study the immune-modulatory role of IFN- $\lambda$  in B cells. We performed transcriptomics on B cells to study their response to IFN- $\lambda$ . We have shown the systematic link of how IFN- $\lambda$  enhances B cell differentiation by boosting mTORC1 signaling and the cell-cycle process in BCR-activated cells.

We initially performed a broad analysis to identify which immune cells express a functional IFN- $\lambda$  receptor to resolve the discrepancies in reported data for IFN- $\lambda$  receptor expression on immune cell populations. We clearly showed that IFN- $\lambda$  does not induce STAT1 phosphorylation on NK cells, monocytes, and T cells. Previously, NK cells have been shown not to be directly affected by IFN- $\lambda$  and instead to be affected by IFN- $\lambda$ -stimulated alveolar macrophages (Morrison et al., 2014; Wang et al., 2017). However, the expression of the IFN- $\lambda$  receptor on T cells and

### Figure 3. IFN- $\lambda$ Increases BCR-Induced Cell-Cycle Progression in B Cells

(A and B) Hallmark gene set enrichment barcode plot showing the set of genes from the E2F targets and G2M checkpoints that were upregulated by IFN- $\lambda$ 3 or  $\alpha$ -IgM + IFN- $\lambda$ 3 compared with the  $\alpha$ -IgM alone condition (E2F targets, FDR =  $5.44E-19$ ; G2M checkpoints, FDR =  $1.17E-15$ ). (C) Gene Ontology (GO) enrichment analysis presented the upregulation of cell-cycle-related biological processes (top 20 listed) by IFN- $\lambda$ 3 in BCR-primed B cells. (D) Intracellular Ki-67 expression was measured by flow cytometry after 4 days. The percentages of Ki-67<sup>+</sup> cells are shown in representative FACS plots, and collective results are shown in a scatterplot (n = 4). An ANOVA (Kruskal-Wallis) test with BKY correction was used to determine the significance. (E) Checkpoint inhibitor assay was performed to confirm stimuli-specific induction of B cell proliferation. CTV-labeled B cells were cultured in the presence of IFN- $\lambda$ 3,  $\alpha$ -IgM, or  $\alpha$ -IgM + IFN- $\lambda$ 3 for 5 days. The proliferation of B cells was analyzed by flow cytometry. The percentages of proliferating B cells are shown in representative FACS plots, and the collective results are shown in a scatterplot. Bars show median with IQR. Significance was determined by an ANOVA (Kruskal-Wallis) test with BKY correction.

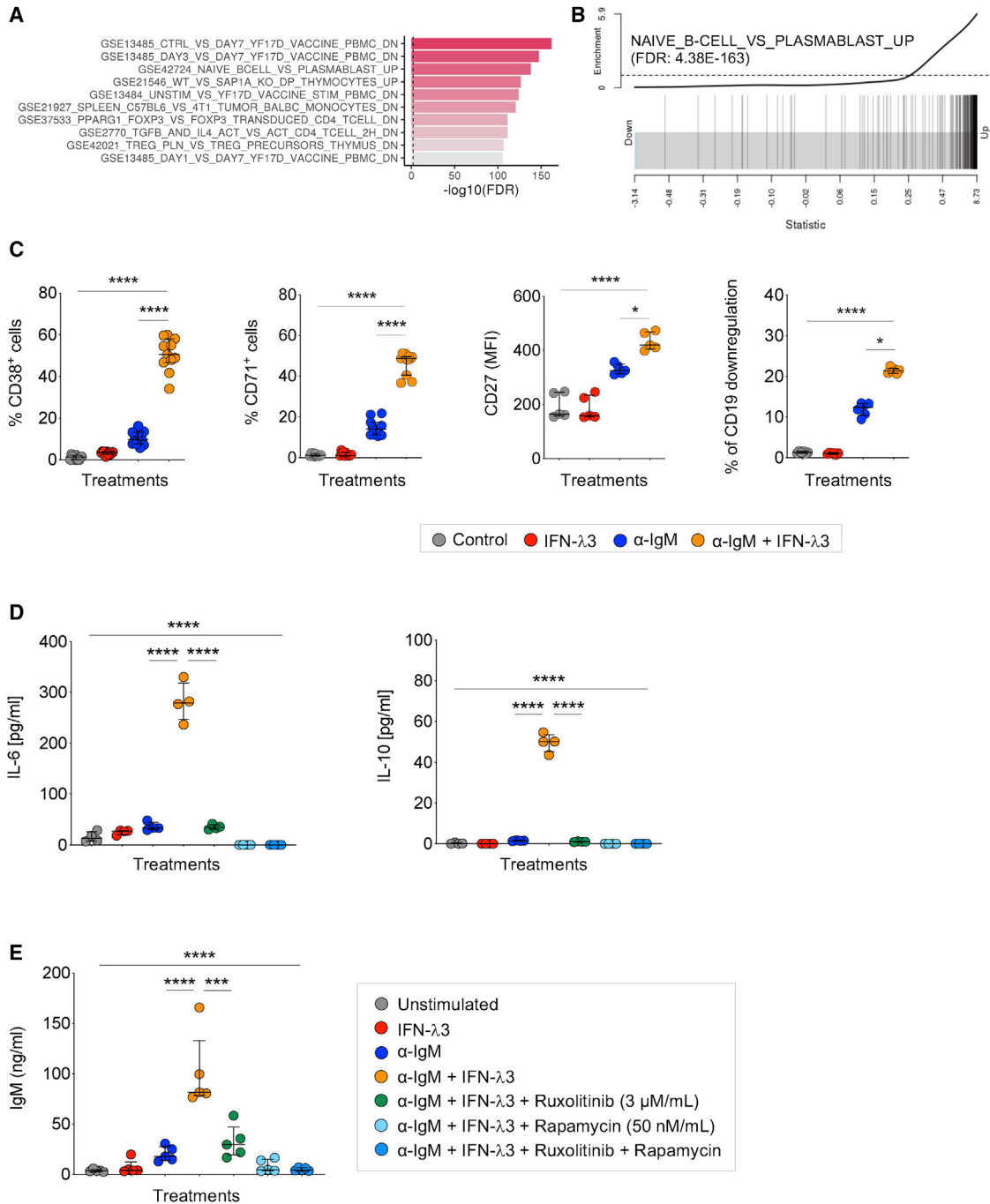


**Figure 4. Effect of IFN-λ on Differentiation of Naive B Cells into Plasmablasts**

(A) List of top 10 pathways upregulated by IFN-λ in B cells over IgM stimulation from hallmark gene set enrichment analysis of immunological signature categories. (B) Hallmark gene set enrichment barcode plot showing that the candidate genes involved in the differentiation of the naive-to-plasmablast process were strongly upregulated by IFN-λ in BCR-primed B cells (FDR = 4.38E-163, α-IgM + IFN-λ3 versus α-IgM). (C) Sorted naive B cells were stimulated with IFN-λ3, α-IgM, or the combination of α-IgM and IFN-λ3 for 4 days. Flow cytometry analysis was performed to measure the upregulation or downregulation of surface markers CD38, CD71, CD19 (percentage of positive cells), and CD27 (in geometric mean fluorescence). (D) For cytokine release, the sorted naive B cells were cultured with IFN-λ3, α-IgM, or the combination of α-IgM and IFN-λ3 with or without JAK or mTORC1 inhibitors. The supernatants were harvested at 72 h. The cytokines were measured by a human B cell cytokine multi-analyte flow assay kit. (E) Sorted naive B cells were treated with the previously indicated conditions, and supernatants were collected on day 5. The released Ig was measured using a human Ig isotyping multi-analyte flow assay kit. Data are shown as median with IQR. Statistical significance was determined by an ANOVA and post-Tukey's test with BKY correction: \*p < 0.05, \*\*p < 0.01, \*\*\*p < 0.001.

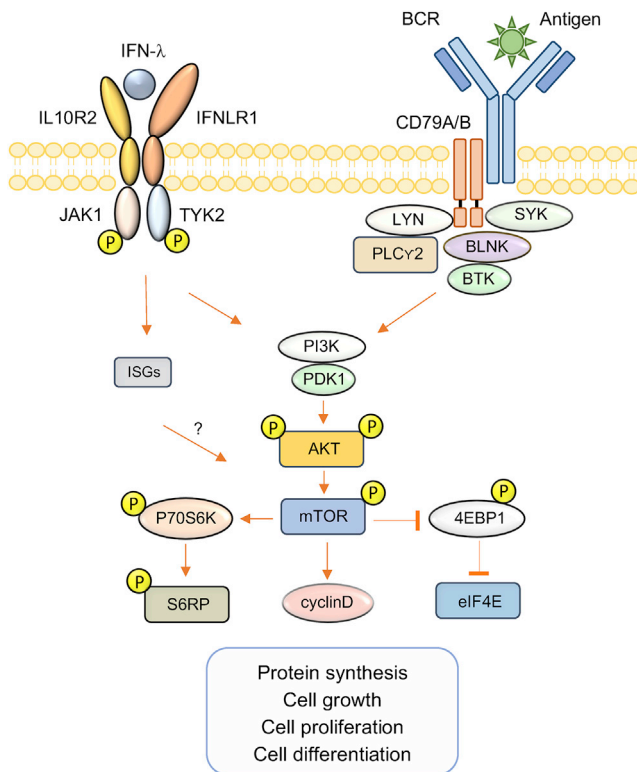


**Figure 5. IFN-λ Synergizes with BCR Signaling through the mTORC1 Pathway**

Schematic illustrates how IFN-λ synergizes with BCR signaling through the mTORC1 pathway to enhance the differentiation of naive B cells into plasmablasts and follow up effector functions.

monocytes has been under debate (Dai et al., 2009; de Groen et al., 2015; Dickensheets et al., 2013; Gallagher et al., 2010; Kelly et al., 2016; Witte et al., 2009). The activation and differentiation states of the immune cells might influence the expression of the IFN-λ receptor. In agreement with previously published data (Kelly et al., 2016; Megjugorac et al., 2009), we observed a strong response of pDCs to IFN-λ. The expression of IFNLR1 mRNA was described for B cells (de Groen et al., 2015; Kelly et al., 2016). We showed the direct responsiveness of B cells to IFN-λ via different functional assays (phospho-flow assay, western blot, and transcriptome profiling by RNA-seq). IFN-λ induces STAT1 phosphorylation in a dose-dependent manner in B cells. Although all B cell subtypes directly respond to IFN-λ, the naive B cell response is about one-fold higher compared with that of memory B cells (Figure S1F). Moreover, IFN-λ-induced gene expression increased over 72 h. In particular, IFN-λ induced the expression of MX1- and leukocyte-recruiting chemokines such as CXCL9, CXCL10, and CXCL11 in B cells. Recent studies have shown that IFN-λ does not induce the expression of MX1 in neutrophils or CXCL9, CXCL10, and CXCL11 in A549 human airway epithelial cells and hepatocytes (PH5CH8) (Forero et al., 2019; Galani et al., 2017). Overall, our results show that IFN-λ signaling is steady and prolonged, as in hepatocytes (Forero et al., 2019); at the same time, IFN-λ-induced gene expression can be cell type specific.

The metabolic regulator mTORC1 has a crucial role in B cell-fate decision and immune response (Kwak et al., 2019). Our B cell transcriptomics and follow-up *in vitro* experimental data indicate that IFN-λ boosts the mTORC1 pathway upon BCR activation in B cells. IFN-λ significantly increased the BCR-induced phosphorylation of S6, like IFN-α. In addition, type I IFNs have been previously shown to upregulate Toll-like receptor (TLR)-induced mTORC1 activity on B cells and their subpopulations (Torigo et al., 2017). It is known that type III IFN downstream signaling has delayed kinetics compared with type I IFNs (Jilg et al., 2014; Marcello et al., 2006). Our data indicate that IFN-λ-induced mTORC1 signaling is initially (up to 8 h) delayed in BCR-activated cells compared with IFN-α; however, it catches the S6 phosphorylation kinetics over time (at 16 h) (Figure 2B; Figure S2D). Furthermore, JAK inhibition confirms IFN-λ-specific enhancement of the mTORC1 pathway. The engagement of mTORC1 by BCR and the IFN-λ receptor takes place via PI3K, which is confirmed by inhibition of PI3K. Similar to type I IFNs, type III IFNs may induce the mTORC1 pathway by activating PI3K via JAKs in an IRS-dependent but STAT-independent manner (Platanias, 2005).

mTORC1/S6 plays an important role in cell-cycle progression (Wullschlegel et al., 2006). Ongoing mTORC1 signaling and cell-cycle progression lead to cellular differentiation. mTORC1 signaling is known to be involved in immune cell differentiation (Jones and Pearce, 2017; Sukhbaatar et al., 2016). Our B cell transcriptomics and follow-up *in vitro* experimental data suggest that upon BCR activation, IFN-λ boosts cell-cycle progress by enhancing the mTORC1 pathway and that it leads to differentiation of naive B cells into plasmablasts with gained effector functions such as cytokine and antibody release. Although IFN-λ alone could slightly enrich mTORC1 and cell-cycle (E2F and G2M) gene expression at 72 h (Table S2), our *in vitro* data show that the effect of IFN-λ alone on mTORC1 signaling and cell proliferation is limited. The effect is heightened significantly only when IFN-λ is added with BCR activation. Because IFN-λ could induce more pSTAT1 in naive B cells, IFN-λ-enhanced proliferation of BCR-activated naive B cells is potentially higher compared with memory B cells (Figures S1F and S3D). Jago et al. (2003) clearly demonstrated the role of type I IFNs and IL-6 in a distinct stage of B cell differentiation. Similar to type I IFNs, IFN-λ boosts plasmablast differentiation of BCR-activated naive B cells. Our experiment shows that IFN-λ increased the expression IL-6R, as well as the release of IL-6 cytokine after day 3. Therefore, it may play a major role in the next stage of differentiation from plasmablasts into plasma cells.

Our data suggest that no class switching takes place in naive B cells in 5 days of stimulation. The cytokine IL-21 induces the naive B cell differentiation via strong STAT3 activation with a dispensable STAT1 function. (Avery et al., 2010). IFN-λ-induced phosphorylation of signal transducer and activator of transcription 3 (pSTAT3) needs to be evaluated in B cell subpopulations to understand the class-switching capability of IFN-λ on activated B cells. Furthermore, the release of IgA and IgG1 from total or memory B cells might result from the activation of class-switched memory cells, which are already present in their populations.

Although mouse B cells lack the IFN-λ receptor, IFN-λ indirectly triggers the germinal center reaction and antibody production by a mechanism dependent on thymic stromal lymphopoietin (TSLP)

(Ye et al., 2019). In humans, the mechanistic role of IFN- $\lambda$  in humoral immunity needs to be further evaluated in a precise context and a properly defined environment. The further role of IFN- $\lambda$ -induced ISGs in mTORC1 activity and follow-up functions can be explored (Figure 5). The role of IFN- $\lambda$  in autoimmune diseases is not well established yet. However, IFN- $\lambda$  has been shown to be positively correlated with induction of pro-inflammatory cytokines (IL-6, IL-8, IL-10, and CXCL9), as well as anti-nucleosome, anti-double strand DNA (anti-dsDNA) antibodies in systemic lupus erythematosus (SLE) patients, and to be associated with pathogenesis of lupus nephritis (LN) (Vlachiotis and Andreakos, 2019; Zickert et al., 2016). Furthermore, the level of pmTORC1 in CD19<sup>+</sup> B cells positively correlated with the number of peripheral plasmablasts and the SLE disease activity score index (Torigoe et al., 2017). To connect our findings with previous clinical observations, the role of IFN- $\lambda$  signaling might be interesting to evaluate in hyperactive B cell in the development of SLE and LN.

In conclusion, our work demonstrates the direct response of B cells to IFN- $\lambda$ . Furthermore, it reveals how IFN- $\lambda$  systematically boosts plasmablast differentiation by enhancing the mTORC1 pathway and cell-cycle progression in activated B cells (Figure 5). These findings are particularly important in the context of IFN- $\lambda$  signaling as a potential therapeutic target. Our data have provided insight into the molecular mechanisms behind the immune-modulatory function of IFN- $\lambda$  signaling in B cells, which might help the optimization of vaccine efficacies and improve strategies to target B cell-associated autoimmune and infectious disease treatment.

## STAR★METHODS

Detailed methods are provided in the online version of this paper and include the following:

- KEY RESOURCES TABLE
- RESOURCE AVAILABILITY
  - Lead Contact
  - Materials Availability
  - Data and Code Availability
- EXPERIMENTAL MODEL AND SUBJECT DETAILS
  - Human B cells preparation and culture
- METHOD DETAILS
  - pSTAT1/2 or Mx1 measurement
  - Immunoblotting
  - mTORC1 inhibitor assay
  - Ki-67 measurement
  - TaqMAN gene expression assay
  - B cell proliferation assay
  - Measurement of surface markers for naive to plasmablast differentiation
  - Immunoglobulins and cytokines measurement
  - B cell transcriptomics
- QUANTIFICATION AND STATISTICAL ANALYSIS

## SUPPLEMENTAL INFORMATION

Supplemental Information can be found online at <https://doi.org/10.1016/j.celrep.2020.108211>.

## ACKNOWLEDGMENTS

We thank Dr. Peter Staeheli, Institute of Virology, Medical Center University of Freiburg, Germany, for providing the Mx1 antibody. We thank the Flow cytometry core facility (Department of Biomedicine) and sciCORE (<http://scicore.unibas.ch>) scientific computing facility at the University of Basel. We thank Functional Genomics Center Zurich (FGCZ) (<https://fgcz.ch>). We thank Dominik Vogt for technical assistance. We thank Dr. Helena Seth-Smith for critical reading of the manuscript. This work was supported by a research grant to AE Swiss National Science Foundation (project grant PZ00P3\_154709/1) and the Swiss National Science Foundation SystemsX iPhD program. In addition, grants came from the Nachwuchsförderung Universität Basel, Bangerter Rhyner Stiftung, and Stiftung für Infektionskrankheiten.

## AUTHOR CONTRIBUTIONS

M.S., F.B., J.L., C.S., D.W., and A.E. designed the experiments. M.S. performed the experiments. M.S. performed analysis of immunoblotting data. M.S. and J.L. performed analysis of flow cytometry data. F.B. performed analysis of transcriptomics data. M.S. and A.E. wrote the initial draft of the manuscript, with the other authors providing editorial comments.

## DECLARATION OF INTERESTS

The authors declare no competing interests.

Received: October 17, 2019

Revised: June 24, 2020

Accepted: September 9, 2020

Published: October 6, 2020

## REFERENCES

- Ank, N., Iversen, M.B., Bartholdy, C., Staeheli, P., Hartmann, R., Jensen, U.B., Dagnaes-Hansen, F., Thomsen, A.R., Chen, Z., Haugen, H., et al. (2008). An important role for type III interferon (IFN- $\lambda$ /IL-28) in TLR-induced antiviral activity. *J. Immunol.* *180*, 2474–2485.
- Avery, D.T., Deenick, E.K., Ma, C.S., Suryani, S., Simpson, N., Chew, G.Y., Chan, T.D., Palendira, U., Bustamante, J., Boisson-Dupuis, S., et al. (2010). B cell-intrinsic signaling through IL-21 receptor and STAT3 is required for establishing long-lived antibody responses in humans. *J. Exp. Med.* *207*, 155–171.
- Benjamini, Y., Krieger, A.M., and Yekutieli, D. (2006). Adaptive Linear Step-up Procedures That Control the False Discovery Rate. *Biometrika* *93*, 491–507.
- Broggi, A., Tan, Y., Granucci, F., and Zanoni, I. (2017). IFN- $\lambda$  suppresses intestinal inflammation by non-translational regulation of neutrophil function. *Nat. Immunol.* *18*, 1084–1093.
- Caine, E.A., Scheaffer, S.M., Arora, N., Zaitsev, K., Artyomov, M.N., Coyne, C.B., Moley, K.H., and Diamond, M.S. (2019). Interferon lambda protects the female reproductive tract against Zika virus infection. *Nat. Commun.* *10*, 280.
- Chen, S., Zhou, Y., Chen, Y., and Gu, J. (2018). fastp: an ultra-fast all-in-one FASTQ preprocessor. *Bioinformatics* *34*, i884–i890.
- Chevrier, S., Genton, C., Kallies, A., Karnowski, A., Otten, L.A., Malissen, B., Malissen, M., Botto, M., Corcoran, L.M., Nutt, S.L., and Acha-Orbea, H. (2009). CD93 is required for maintenance of antibody secretion and persistence of plasma cells in the bone marrow niche. *Proc. Natl. Acad. Sci. USA* *106*, 3895–3900.
- Dai, J., Megjugorac, N.J., Gallagher, G.E., Yu, R.Y., and Gallagher, G. (2009). IFN- $\lambda$ 1 (IL-29) inhibits GATA3 expression and suppresses Th2 responses in human naive and memory T cells. *Blood* *113*, 5829–5838.
- Darzynkiewicz, Z., Zhao, H., Zhang, S., Lee, M.Y., Lee, E.Y., and Zhang, Z. (2015). Initiation and termination of DNA replication during S phase in relation to cyclins D1, E and A, p21WAF1, Cdt1 and the p12 subunit of DNA polymerase  $\delta$  revealed in individual cells by cytometry. *Oncotarget* *6*, 11735–11750.

- de Groen, R.A., Groothuisink, Z.M., Liu, B.S., and Boonstra, A. (2015). IFN- $\lambda$  is able to augment TLR-mediated activation and subsequent function of primary human B cells. *J. Leukoc. Biol.* **98**, 623–630.
- Dickensheets, H., Sheikh, F., Park, O., Gao, B., and Donnelly, R.P. (2013). Interferon-lambda (IFN- $\lambda$ ) induces signal transduction and gene expression in human hepatocytes, but not in lymphocytes or monocytes. *J. Leukoc. Biol.* **93**, 377–385.
- Dobin, A., Davis, C.A., Schlesinger, F., Drenkow, J., Zaleski, C., Jha, S., Batut, P., Chaisson, M., and Gingeras, T.R. (2013). STAR: ultrafast universal RNA-seq aligner. *Bioinformatics* **29**, 15–21.
- Dowling, R.J., Topisirovic, I., Alain, T., Bidinosti, M., Fonseca, B.D., Petroulakis, E., Wang, X., Larsson, O., Selvaraj, A., Liu, Y., et al. (2010). mTORC1-mediated cell proliferation, but not cell growth, controlled by the 4E-BPs. *Science* **328**, 1172–1176.
- Doyle, S.E., Schreckhise, H., Khuu-Duong, K., Henderson, K., Rosler, R., Storey, H., Yao, L., Liu, H., Barahmand-pour, F., Sivakumar, P., et al. (2006). Interleukin-29 uses a type 1 interferon-like program to promote antiviral responses in human hepatocytes. *Hepatology* **44**, 896–906.
- Egli, A., Santer, D.M., O’Shea, D., Tyrrell, D.L., and Houghton, M. (2014). The impact of the interferon-lambda family on the innate and adaptive immune response to viral infections. *Emerg. Microbes Infect.* **3**, e51.
- Ellebedy, A.H., Jackson, K.J., Kissick, H.T., Nakaya, H.I., Davis, C.W., Roskin, K.M., McElroy, A.K., Oshansky, C.M., Elbein, R., Thomas, S., et al. (2016). Defining antigen-specific plasmablast and memory B cell subsets in human blood after viral infection or vaccination. *Nat. Immunol.* **17**, 1226–1234.
- Forero, A., Ozarkar, S., Li, H., Lee, C.H., Hemann, E.A., Nadjombati, M.S., Hendricks, M.R., So, L., Green, R., Roy, C.N., et al. (2019). Differential Activation of the Transcription Factor IRF1 Underlies the Distinct Immune Responses Elicited by Type I and Type III Interferons. *Immunity* **51**, 451–464.
- Fruman, D.A., Chiu, H., Hopkins, B.D., Bagrodia, S., Cantley, L.C., and Abraham, R.T. (2017). The PI3K Pathway in Human Disease. *Cell* **170**, 605–635.
- Galani, I.E., Triantafyllia, V., Eleminiadou, E.E., Koltsida, O., Stavropoulos, A., Manioudaki, M., Thanos, D., Doyle, S.E., Kottenko, S.V., Thanopoulou, K., et al. (2017). Interferon- $\lambda$  Mediates Non-redundant Front-Line Antiviral Protection against Influenza Virus Infection without Compromising Host Fitness. *Immunity* **46**, 875–890.
- Gallagher, G., Megjugorac, N.J., Yu, R.Y., Eskdale, J., Gallagher, G.E., Siegel, R., and Tollar, E. (2010). The lambda interferons: guardians of the immune-epithelial interface and the T-helper 2 response. *J. Interferon Cytokine Res.* **30**, 603–615.
- Haller, O., Arnheiter, H., Pavlovic, J., and Staeheli, P. (2018). The Discovery of the Antiviral Resistance Gene Mx: A Story of Great Ideas, Great Failures, and Some Success. *Annu. Rev. Virol.* **5**, 33–51.
- Hay, N., and Sonenberg, N. (2004). Upstream and downstream of mTOR. *Genes Dev.* **18**, 1926–1945.
- Hemann, E.A., Green, R., Turnbull, J.B., Langlois, R.A., Savan, R., and Gale, M., Jr. (2019). Interferon- $\lambda$  modulates dendritic cells to facilitate T cell immunity during infection with influenza A virus. *Nat. Immunol.* **20**, 1035–1045.
- Horvath, C.M. (2004). The Jak-STAT pathway stimulated by interferon alpha or interferon beta. *Sci. STKE* **2004**, tr10.
- Jego, G., Palucka, A.K., Blanck, J.P., Chalouni, C., Pascual, V., and Banchereau, J. (2003). Plasmacytoid dendritic cells induce plasma cell differentiation through type I interferon and interleukin 6. *Immunity* **19**, 225–234.
- Jilg, N., Lin, W., Hong, J., Schaefer, E.A., Wolski, D., Meixong, J., Goto, K., Brisac, C., Chusri, P., Fusco, D.N., et al. (2014). Kinetic differences in the induction of interferon stimulated genes by interferon- $\alpha$  and interleukin 28B are altered by infection with hepatitis C virus. *Hepatology* **59**, 1250–1261.
- Jones, R.G., and Pearce, E.J. (2017). mTORing Immunity: mTOR Signaling in the Development and Function of Tissue-Resident Immune Cells. *Immunity* **46**, 730–742.
- Kelly, A., Robinson, M.W., Roche, G., Biron, C.A., O’Farrelly, C., and Ryan, E.J. (2016). Immune Cell Profiling of IFN- $\lambda$  Response Shows pDCs Express Highest Level of IFN- $\lambda$ R1 and Are Directly Responsive via the JAK-STAT Pathway. *J. Interferon Cytokine Res.* **36**, 671–680.
- Kwak, K., Akkaya, M., and Pierce, S.K. (2019). B cell signaling in context. *Nat. Immunol.* **20**, 963–969.
- Kwon, H., Thierry-Mieg, D., Thierry-Mieg, J., Kim, H.P., Oh, J., Tunyaplin, C., Carotta, S., Donovan, C.E., Goldman, M.L., Taylor, P., et al. (2009). Analysis of interleukin-21-induced Prdm1 gene regulation reveals functional cooperation of STAT3 and IRF4 transcription factors. *Immunity* **31**, 941–952.
- Lazear, H.M., Daniels, B.P., Pinto, A.K., Huang, A.C., Vick, S.C., Doyle, S.E., Gale, M., Jr., Klein, R.S., and Diamond, M.S. (2015). Interferon- $\lambda$  restricts West Nile virus neuroinvasion by tightening the blood-brain barrier. *Sci. Transl. Med.* **7**, 284ra59.
- Lou, Z., Casali, P., and Xu, Z. (2015). Regulation of B Cell Differentiation by Intracellular Membrane-Associated Proteins and microRNAs: Role in the Antibody Response. *Front. Immunol.* **6**, 537.
- Marcello, T., Grakoui, A., Barba-Spaeth, G., Machlin, E.S., Kottenko, S.V., MacDonald, M.R., and Rice, C.M. (2006). Interferons alpha and lambda inhibit hepatitis C virus replication with distinct signal transduction and gene regulation kinetics. *Gastroenterology* **131**, 1887–1898.
- McCarthy, D.J., and Smyth, G.K. (2009). Testing significance relative to a fold-change threshold is a TREAT. *Bioinformatics* **25**, 765–771.
- Megjugorac, N.J., Gallagher, G.E., and Gallagher, G. (2009). Modulation of human plasmacytoid DC function by IFN-lambda1 (IL-29). *J. Leukoc. Biol.* **86**, 1359–1363.
- Moens, L., and Tangye, S.G. (2014). Cytokine-Mediated Regulation of Plasma Cell Generation: IL-21 Takes Center Stage. *Front. Immunol.* **5**, 65.
- Morrison, M.H., Keane, C., Quinn, L.M., Kelly, A., O’Farrelly, C., Bergin, C., and Gardiner, C.M. (2014). IFNL cytokines do not modulate human or murine NK cell functions. *Hum. Immunol.* **75**, 996–1000.
- Munakata, W., and Tobinai, K. (2018). Clinical development of vortalisib: a pan-PI3K/mTOR inhibitor. *Lancet Haematol.* **5**, e134–e135.
- Nice, T.J., Baldrige, M.T., McCune, B.T., Norman, J.M., Lazear, H.M., Artyomov, M., Diamond, M.S., and Virgin, H.W. (2015). Interferon- $\lambda$  cures persistent murine norovirus infection in the absence of adaptive immunity. *Science* **347**, 269–273.
- Platanias, L.C. (2005). Mechanisms of type-I- and type-II-interferon-mediated signalling. *Nat. Rev. Immunol.* **5**, 375–386.
- Pott, J., Mhlaköv, T., Mordstein, M., Duerr, C.U., Michiels, T., Stockinger, S., Staeheli, P., and Hornef, M.W. (2011). IFN-lambda determines the intestinal epithelial antiviral host defense. *Proc. Natl. Acad. Sci. USA* **108**, 7944–7949.
- R Core Team (2013). R: A language and environment for statistical computing (R Foundation for Statistical Computing).
- Ritchie, M.E., Phipson, B., Wu, D., Hu, Y., Law, C.W., Shi, W., and Smyth, G.K. (2015). limma powers differential expression analyses for RNA-sequencing and microarray studies. *Nucleic Acids Res.* **43**, e47.
- Robinson, M.D., McCarthy, D.J., and Smyth, G.K. (2010). edgeR: a Bioconductor package for differential expression analysis of digital gene expression data. *Bioinformatics* **26**, 139–140.
- Schneider, W.M., Chevillotte, M.D., and Rice, C.M. (2014). Interferon-stimulated genes: a complex web of host defenses. *Annu. Rev. Immunol.* **32**, 513–545.
- Subramanian, A., Tamayo, P., Mootha, V.K., Mukherjee, S., Ebert, B.L., Gillette, M.A., Paulovich, A., Pomeroy, S.L., Golub, T.R., Lander, E.S., and Mesirov, J.P. (2005). Gene set enrichment analysis: a knowledge-based approach for interpreting genome-wide expression profiles. *Proc. Natl. Acad. Sci. USA* **102**, 15545–15550.
- Sukhbaatar, N., Hengstschläger, M., and Weichhart, T. (2016). mTOR-Mediated Regulation of Dendritic Cell Differentiation and Function. *Trends Immunol.* **37**, 778–789.
- Syedbasha, M., and Egli, A. (2017). Interferon Lambda: Modulating Immunity in Infectious Diseases. *Front. Immunol.* **8**, 119.

- Tellier, J., Shi, W., Minnich, M., Liao, Y., Crawford, S., Smyth, G.K., Kallies, A., Busslinger, M., and Nutt, S.L. (2016). Blimp-1 controls plasma cell function through the regulation of immunoglobulin secretion and the unfolded protein response. *Nat. Immunol.* *17*, 323–330.
- Torigoe, M., Iwata, S., Nakayama, S., Sakata, K., Zhang, M., Hajime, M., Miyazaki, Y., Narisawa, M., Ishii, K., Shibata, H., and Tanaka, Y. (2017). Metabolic Reprogramming Commits Differentiation of Human CD27<sup>+</sup>IgD<sup>+</sup> B Cells to Plasmablasts or CD27<sup>-</sup>IgD<sup>-</sup> Cells. *J. Immunol.* *199*, 425–434.
- Vlachiotis, S., and Andreakos, E. (2019). Lambda interferons in immunity and autoimmunity. *J. Autoimmun.* *104*, 102319.
- Wack, A., Terczyńska-Dyla, E., and Hartmann, R. (2015). Guarding the frontiers: the biology of type III interferons. *Nat. Immunol.* *16*, 802–809.
- Wang, Y., Li, T., Chen, Y., Wei, H., Sun, R., and Tian, Z. (2017). Involvement of NK Cells in IL-28B-Mediated Immunity against Influenza Virus Infection. *J. Immunol.* *199*, 1012–1020.
- Witte, K., Gruetz, G., Volk, H.D., Looman, A.C., Asadullah, K., Sterry, W., Sabaat, R., and Wolk, K. (2009). Despite IFN-lambda receptor expression, blood immune cells, but not keratinocytes or melanocytes, have an impaired response to type III interferons: implications for therapeutic applications of these cytokines. *Genes Immun.* *10*, 702–714.
- Wu, D., and Smyth, G.K. (2012). Camera: a competitive gene set test accounting for inter-gene correlation. *Nucleic Acids Res.* *40*, e133.
- Wullschlegel, S., Loewith, R., and Hall, M.N. (2006). TOR signaling in growth and metabolism. *Cell* *124*, 471–484.
- Ye, L., Schnepf, D., Becker, J., Ebert, K., Tanriver, Y., Bernasconi, V., Gad, H.H., Hartmann, R., Lycke, N., and Staeheli, P. (2019). Interferon- $\lambda$  enhances adaptive mucosal immunity by boosting release of thymic stromal lymphopoietin. *Nat. Immunol.* *20*, 593–601.
- Zhang, S., Kodys, K., Li, K., and Szabo, G. (2013). Human type 2 myeloid dendritic cells produce interferon- $\lambda$  and amplify interferon- $\alpha$  in response to hepatitis C virus infection. *Gastroenterology* *144*, 414–425.
- Zickert, A., Oke, V., Parodis, I., Svenungsson, E., Sundström, Y., and Gunnarsson, I. (2016). Interferon (IFN)- $\lambda$  is a potential mediator in lupus nephritis. *Lupus Sci. Med.* *3*, e000170.

STAR★METHODS

KEY RESOURCES TABLE

REAGENT or RESOURCE	SOURCE	IDENTIFIER
<b>Antibodies</b>		
CD3-BV785 (OKT3)	BioLegend	Cat# 317330; RRID:AB_2563507
CD4-FITC (SK3)	BioLegend	Cat# 344604; RRID:AB_1937227
CD14-PE (M5E2)	BioLegend	Cat# 301806; RRID:AB_314188
CD19-APC (SJ25C1)	BioLegend	Cat# 363006; RRID:AB_2564128
CD19-PE/Cy7 (H1B19)	BioLegend	Cat# 302216; RRID:AB_314246
CD27-BV421 (M-T271)	BioLegend	Cat# 356418; RRID:AB_2562599
CD27-PE (M-T271)	BioLegend	Cat# 356406; RRID:AB_2561825
IgD-BV605 (IA6-2)	BioLegend	Cat# 348232; RRID:AB_2563337
CD38-BV711 (HIT2)	BioLegend	Cat# 303528; RRID:AB_2563811
IgM-PE/Cy7 (MHM-88)	BioLegend	Cat# 314531; RRID:AB_2566484
CD8-PE/Cy7 (SK1)	BioLegend	Cat# 344712; RRID:AB_2044008
CD123-PE/Cy7 (6H6)	BioLegend	Cat# 306009; RRID:AB_493577
BDCA-2-BV421 (201A)	BioLegend	Cat# 354211; RRID:AB_2562320
CD38-APC/Cy7 (HIT2)	BioLegend	Cat# 303533; RRID:AB_2561604
CD335-BV605 (9E2)	BioLegend	Cat# 331926; RRID:AB_2563855
CD71-APC/Cy7 (CY1G4)	BioLegend	Cat# 334109; RRID:AB_2563116
Ki-67-BV421 (Ki-67)	BioLegend	Cat# 350506; RRID:AB_2563860
Anti-Mouse-AF-647 (Poly4053)	BioLegend	Cat# 405322; RRID:AB_2563045
Stat1-pY701-AF647 (4a)	BD Biosciences	Cat# 612597; RRID:AB_399880
S6-pS235/p236-AF488 (N7-548)	BD Biosciences	Cat# 560434
mTOR-(pS2448)-AF647 (021-404)	BD Biosciences	Cat# 564242; RRID:AB_2738695
Anti-Rabbit-AF647	Cell Signaling technology	Cat# 4414S; RRID:AB_10693544
HRP-anti-Rabbit Ab	Cell Signaling technology	Cat# 7074S; RRID:AB_2099233
pSTAT1 (Tyr701) Rabbit mAb (58D6)	Cell Signaling technology	Cat# 9167S; RRID:AB_561284
pSTAT2 (Thr690) Rabbit mAb (58D6)	Cell Signaling technology	Cat# 90740S; RRID:AB_2800162
p4EBP1 (T37/46) Rabbit mAb (236B4)	Cell Signaling technology	Cat# 2855S; RRID:AB_560835
Monoclonal anti-β-Actin antibody (mouse)	Sigma Aldrich	Cat# A5441; RRID:AB_476744
HRP-goat-anti-mouse Ab	Jackson Immuno Research	Cat# 115-035-166; RRID:AB_2338511
Affinipure F(ab') <sub>2</sub> goat-anti-human IgM	Jackson Immuno Research	Cat# 109-006-129; RRID:AB_2337553
Affinipure F(ab') <sub>2</sub> goat-anti-human IgG	Jackson Immuno Research	Cat# 109-006-088; RRID:AB_2337549
mouse anti- human Mx1	Gift from Dr. Peter Staeheli	N/A
<b>Biological Samples</b>		
Human blood	Blood donation center, University Hospital Basel	N/A
<b>Chemicals, Peptides, and Recombinant Proteins</b>		
4X Laemmli sample buffer	Bio-Rad	Cat# 161-0747
Super signal West Pico chemiluminescent	Thermo Fisher Scientific	Cat# 34080
Bovine Serum Albumin	Sigma Aldrich	Cat# A7906
Tween20	Sigma Aldrich	Cat# P7949
Nitrocellulose membrane	GE Healthcare Life Sciences	Cat# 10600016
Fix Buffer I	BD Biosciences	Cat# 557870
Perm Buffer III	BD Biosciences	Cat# 558050
Recombinant Human IL-29/IFN-lambda 1 Protein	R&D SYSTEMS	Cat# 1598-IL-025/CF

(Continued on next page)

**Continued**

REAGENT or RESOURCE	SOURCE	IDENTIFIER
Recombinant Human IL-28A/IFN-lambda 2 Protein	R&D SYSTEMS	Cat# 1587-IL-025/CF
Recombinant Human IL-28B/IFN-lambda 3 Protein	R&D SYSTEMS	Cat# 5259-IL-025/CF
Ruxolitinib	Selleckchem	Cat# S1378
Wortmannin	Selleckchem	Cat# S2758
Rapamycin	Selleckchem	Cat# S1039
Critical Commercial Assays		
EasySep Human B Cell Enrichment Kit	STEMCELL Technologies	Cat# 19054
RNeasy Micro Kit	QIAGEN	Cat# 74004
High-Capacity cDNA Reverse Transcription Kit	Applied Biosystems	Cat# 4368814
TaqMan Universal PCR Master Mix	Applied Biosystems	Cat# 4324018
ACIDA - TaqMan Gene Expression Assays	Thermo Fisher Scientific	Cat# Hs00757808_m1
PRDM1 - TaqMan Gene Expression Assays	Thermo Fisher Scientific	Cat# Hs00153357_m1
ZombieUV fixable viability kit	BioLegend	Cat# 423108
Zombie Aqua fixable viability kit	BioLegend	Cat# 423102
LEGENDplex Human Ig isotyping panel	BioLegend	Cat# 740638
LEGENDplex Human B cell panel	BioLegend	Cat# 740527
Deposited Data		
B cell RNA sequencing data	This paper	GEO: GSE156195
Software and Algorithms		
FlowJo11	FlowJo LLC	<a href="http://www.flowjo.com">http://www.flowjo.com</a>
Prism	GraphPad Software, Inc	<a href="http://www.graphpad.com">http://www.graphpad.com</a>

**RESOURCE AVAILABILITY**

**Lead Contact**

Further information and requests for resources and reagents should be directed to and will be fulfilled by the Lead Contact, Mohamedyaseen Syedbasha ([m.syedbasha@unibas.ch](mailto:m.syedbasha@unibas.ch)).

**Materials Availability**

This study did not generate new unique reagents.

**Data and Code Availability**

The datasets generated during this study are available at NCBI's Gene Expression Omnibus (GEO) and are accessible through GEO Series accession number GSE156195.

**EXPERIMENTAL MODEL AND SUBJECT DETAILS**

**Human B cells preparation and culture**

Blood samples and buffy coats were collected from healthy blood donors after written informed consent (Blood donor center, University Hospital Basel). PBMCs were isolated from buffy-coats or from whole blood by a ficoll density gradient centrifugation method. B cells were then purified from the PBMC fraction using a negative selection Easysep human B cell enrichment kit (STEMCELL Technologies). A Zombie UV or zombie aqua fixable viability kit was used for live-dead staining according to the manufacturer's instructions (BioLegend). Live CD19<sup>+</sup> B cells were sorted using BD FACS ARIA III cell sorter (BD Biosciences). Sorted B cells were cultured in RPMI 1640 medium (Sigma) supplemented with L-glutamine, 10% heat-inactivated FBS (GIBCO). The cells were incubated at 37°C with 5% CO<sub>2</sub>.

**METHOD DETAILS**

**pSTAT1/2 or Mx1 measurement**

5 × 10<sup>5</sup> PBMCs or isolated B cells were stimulated with IFN- $\alpha$ 2 (1000 U/mL, PBL assay Sciences) or IFN- $\lambda$ 1 (1  $\mu$ g/mL, R&D Systems) for 30 min. The cells were surface stained for 20 min, with following surface markers in different panels 1) For Immune cell

sub-populations: CD19 (PE/Cy7), CD3 (FITC), CD14 (PE), CD335 (Nkp46) (BV605). 2) For pDCs: CD3 (BV-785), CD19 (APC/Cy7), BDCA-2 (BV-421), CD123 (PE/Cy7). 3) For CD4, CD8 T cells: CD4 (FITC), CD8 (PE/Cy7), CD3 (BV-785), CD19 (APC/Cy7). 4) For Isolated B cells CD19 (PE/Cy7), IgD (BV-605), CD27 (BV-421). The cells were fixed with fix buffer I (BD Biosciences) for 10 min at 37°C and permeabilized with perm buffer III (BD Biosciences) for 30 min on ice. After washing, pSTAT1 (AF-647) (BD Biosciences) antibody was added for 1 h, at RT. For pSTAT2 measurement, the fixed and permeabilized cells were incubated with rabbit anti-human pSTAT2 (AF-647) (Cell Signaling Technology, CST) for 1h at RT. For Mx1 measurement, the cells were fixed at 24h. After the permeabilization mouse anti-human Mx1 primary antibody was added for 45 min, at RT. After washing the anti-mouse AF-647 secondary antibody was added for 30 min, at RT. Finally, cells were harvested for flow cytometry analysis. Data were acquired on LSRFortessa (BD Biosciences) and analyzed using FlowJo software (Tree Star Inc).

### Immunoblotting

PBMCs were stimulated with or without IFN- $\alpha$ 2 (1000 U/mL) or IFN- $\lambda$ 1 (1  $\mu$ g/mL) for 30 min. The cells were fixed with fix buffer I (BD Biosciences). The surface markers CD3, CD19, CD335 (Nkp46), and CD14 were used to sort T-, B-, NK-cells, and monocytes respectively by using BD FACS ARIA III cell sorter (BD Biosciences). The sorted immune cell subpopulations were directly lysed in 4X laemmli buffer (Bio-Rad). Proteins were separated by 10% SDS gel electrophoresis and then transferred on to nitrocellulose membranes. The membranes were blocked using 5% BSA in TBST buffer for 1 h, at RT. After washing, pSTAT1 (Cell Signaling Technology, CST) or  $\beta$ -actin (Sigma) primary antibodies were added for overnight incubation at 4°C. After washing with TBST buffer, HRP linked anti-rabbit (CST) or anti-mouse (Jackson Immuno Research) secondary antibody was added, followed by detection with ECL substrate (Thermo Fisher Scientific) using ChemiDoc imaging system (Bio-Rad)

### mTORC1 inhibitor assay

$5 \times 10^5$  isolated B cells were pre-incubated with Ruxolitinib (3  $\mu$ M/mL, JAK1/JAK2 inhibitor) (Selleckchem) or Wortmannin (0.5  $\mu$ M/mL, PI3K inhibitor) (Selleckchem) or Rapamycin (0.05  $\mu$ M/mL, mTORC1 inhibitor) (Selleckchem) for 1 h. After washing, the cells were stimulated with IFN- $\lambda$ 3 (100 ng/mL) (R&D Systems) or  $\alpha$ -IgM (2  $\mu$ g/mL) (IgM Fab'2 fragments from Jackson Immuno Research) or with a combination of  $\alpha$ -IgM and IFN- $\lambda$ 3. The cells were fixed at 16 h with fix buffer I (BD Biosciences) for 10 min at 37°C and permeabilized with perm buffer III (BD Biosciences) for 30 min on ice, after washing anti-human phospho-S6 (Ser235/236, AF-488) (BD Biosciences) or anti-human phospho-mTOR (pS2448, AF-647) (BD Biosciences) antibodies were added for 1 h. For p4EBP1 staining, primary antibody rabbit anti-human phospho-4EBP1 (T37/46) (CST) was added for 45 min. After washing, anti-rabbit (AF-647) secondary antibody (CST) was added for 30 min. Finally, cells were collected for flow cytometry analysis. For immunoglobulin measurements, supernatants were collected after 5 days.

### Ki-67 measurement

$5 \times 10^5$  isolated B cells were stimulated with IFN- $\lambda$ 3 (100 ng/mL)/IFN- $\alpha$ 2 (100 U/mL) or  $\alpha$ -IgM (2  $\mu$ g/mL) or with a combination of  $\alpha$ -IgM and IFN- $\lambda$ 3/ $\alpha$ -IgM and IFN- $\alpha$ 2 for 4 days. After the surface and live-dead staining, cells were fixed with fix buffer I (BD Biosciences) for 10 min at 37°C and permeabilized with perm buffer III (BD Biosciences) for 30 min on ice. After washing, Ki-67 (BV-421) (BioLegend) antibody was added for 45 min at RT. Finally, cells were collected for flow cytometry analysis. Data were acquired on LSRFortessa (BD Biosciences) and analyzed using FlowJo software (Tree Star Inc).

### TaqMAN gene expression assay

The sorted naive or total B cells were stimulated with IFN- $\lambda$ 3 (100 ng/mL),  $\alpha$ -IgM (0.5  $\mu$ g/mL) or  $\alpha$ -IgM + IFN- $\lambda$ 3 for 72 h, approximately  $1 \times 10^6$  cells were used per stimulation condition. After 72 hr the cells were harvested and the total RNA was isolated using the RNeasy micro kit (QIAGEN). cDNA was prepared using high capacity cDNA synthesis reverse transcription Kit (ThermoFisher scientific). The mRNA expression was quantified using 10 ng of cDNA per reaction and HPRT (hypoxanthine phosphoribosyltransferase) was used as a house keeping gene. The following primers from TaqMan gene expression assays were used: HPRT (Hs01003267\_m1), PRDM1 (Hs00153357\_m1), AICDA (Hs00757808\_m1).

### B cell proliferation assay

The sorted total B cells, naive, non-class-switched and class-switched memory B cells were labeled using CTV (Cell Trace Violet) proliferation kit (Thermo Fisher Scientific) according to the manufacturer instructions. CTV labeled total B cells, naive and non-class-switched memory B cells were cultured with IFN- $\lambda$ 3 (100 ng/mL)/IFN- $\alpha$ 2 (100 U/mL) alone or  $\alpha$ -IgM (5  $\mu$ g/mL) alone or with combination of  $\alpha$ -IgM (5  $\mu$ g/mL) and IFN- $\lambda$ 3 (100 ng/mL)/IFN- $\alpha$ 2 (100 U/mL) and the sorted class-switched memory B cells were stimulated with IFN- $\lambda$ 3 (100 ng/mL) or  $\alpha$ -IgG (5  $\mu$ g/mL) or with a combination of  $\alpha$ -IgG and IFN- $\lambda$  for 5 days. The proliferation was measured using LSRFortessa (BD Biosciences) and analyzed using FlowJo software (Tree Star Inc).

### Measurement of surface markers for naive to plasmablast differentiation

$5 \times 10^5$  sorted naive B cells were stimulated with IFN- $\lambda$ 3 (100 ng/mL)/IFN- $\alpha$ 2 (100 U/mL) or  $\alpha$ -IgM (2  $\mu$ g/mL) or with a combination of  $\alpha$ -IgM and IFN- $\lambda$ 3/IFN- $\alpha$ 2 for 4 days. Zombie UV fixable viability kit was used for live-dead staining according to manufacturer

directions (BioLegend). The expressions of surface markers CD27 (BV421), CD71 (APC/Cy7), CD38 (BV711) and CD19(APC/Cy7) (BioLegend) were quantified using LSRTFortessa (BD Biosciences) and analyzed using FlowJo software (Tree Star Inc).

### Immunoglobulins and cytokines measurement

$2 \times 10^5$  sorted total B or naive or non-class-switched memory B cells were stimulated with IFN- $\lambda$ 3 (100 ng/mL)/IFN- $\alpha$ 2 (100 U/mL) or  $\alpha$ -IgM (2  $\mu$ g/mL) or with a combination of  $\alpha$ -IgM and IFN- $\lambda$ 3/IFN- $\alpha$ 2 and sorted class-switched memory B cells were stimulated with IFN- $\lambda$ 3 (100 ng/mL) or  $\alpha$ -IgG (2  $\mu$ g/mL) or with a combination of  $\alpha$ -IgG and IFN- $\lambda$ . The supernatants were collected at 72 h for cytokine measurements. The cytokines were measured using a multi-analyte flow assay (LEGENDplex human B cell cytokines panel, BioLegend). The supernatants were collected at day 5 for immunoglobulin measurements. The immunoglobulins were measured using a multi-analyte flow assay (LEGENDplex human Ig isotyping panel, BioLegend).

### B cell transcriptomics

$1 \times 10^6$  isolated B cells were used per condition, stimulated with IFN- $\lambda$ 3 (100 ng/mL) or  $\alpha$ -IgM (0.5  $\mu$ g/mL) or with a combination of  $\alpha$ -IgM and IFN- $\lambda$ 3. Schematic workflow diagram of the B cell transcriptomics experiment is described in Figure S2B. In total 4 donors were used for IFN- $\lambda$ 3 alone conditions and a total of 6 donors were used for control,  $\alpha$ -IgM and  $\alpha$ -IgM + IFN- $\lambda$ 3 conditions. The total RNA was isolated using the RNeasy micro kit (QIAGEN). The quality of the isolated RNA was determined with a Fragment Analyzer (Agilent, Santa Clara, California, USA). The TruSeq Stranded mRNA kit (Illumina, Inc, California, USA) was used in the subsequent steps. Briefly, total RNA samples (60 ng) were polyA enriched and then reverse-transcribed into double-stranded cDNA. The cDNA samples were fragmented, end-repaired and adenylated before ligation of TruSeq adapters containing unique dual indices (UDI) for multiplexing. Fragments containing TruSeq adapters on both ends were selectively enriched with PCR. The quality and quantity of the enriched libraries were validated using the Fragment Analyzer (Agilent, Santa Clara, California, USA). The product is a smear with an average fragment size of approximately 260 bp. The libraries were normalized to 5 nM in Tris-HCl 10 mM, pH8.5 with 0.1% Tween 20. The Novaseq 6000 (Illumina, Inc, California, USA) was used for cluster generation and sequencing according to the standard protocol (single read, 100 bp). RNA quality control, library preparation, and sequencing were carried out by Functional Genomics Center Zurich (FGCZ) (<https://fgcz.ch>).

The raw RNaseq reads were quality assessed using FastQC v0.11.7 (<http://www.bioinformatics.babraham.ac.uk/projects/fastqc>) and sequencing adaptors trimmed with fastp v0.19.6 (Chen et al., 2018). STAR v2.6.0c was used to align fastq files to the human primary assembly (GRCh37 release 92), and to produce counts of mapped reads per gene (Dobin et al., 2013). Count tables were imported in the R statistical environment and normalized via the TMM method implemented in EdgeR (R Core Team, 2013; Robinson et al., 2010). Genes that had less than 1 count per million (CPM) in more than four samples were filtered out, together with outlier samples identified in principal component analysis (PCA). Genes differentially expressed (DEGs) were independently assessed by fitting a quasi-likelihood negative binomial model and testing the expression in relation to a minimum required log fold-change threshold ( $\log_{FC} = 1.5$ ) (McCarthy and Smyth, 2009). As cutoff for significant DEGs after multiple testing correction (Benjamini-Hochberg - BH), a false discovery rate (FDR) of 1% was used. Smear plots were produced using ggplot2 (<https://ggplot2.tidyverse.org>) and heatmaps generated with pheatmap (<https://cran.r-project.org/web/packages/pheatmap/index.html>).

To test whether a condition was enriched for relevant up/downregulated pathways, the Camera approach was used together with the collection of hallmark and immunologic gene-sets and Gene Ontology (GO) terms from Molecular Signatures Database (MSigDB) (Subramanian et al., 2005). Using gene-wise moderated t-statistics, Camera tests whether a gene-set is highly ranked relative to condition signature in terms of differential expression ( $\log_{FC}$ ), accounting for inter-gene correlation (Wu and Smyth, 2012). To show the enrichment of gene sets among  $\log_{FC}$  ranked genes, barcode plots were produced using the function implemented in the limma package (Ritchie et al., 2015).

### QUANTIFICATION AND STATISTICAL ANALYSIS

Statistical analysis was performed using Graphpad Prism version 7 and R (R Core Team, 2013) as specified in the figure legends. In summary, for  $\log$ -transformed MFI values and  $\log$ -transformed concentrations where normality can be assumed, groups were compared using ANOVA and Tukey's test. Otherwise, groups were compared using Kruskal-Wallis ANOVA and Wilcoxon signed-rank test with multiple testing correction that controls the false discovery rate (Benjamini-Krieger-Yekutieli) when more than two groups were compared (Benjamini et al., 2006).